

APRIL 21, 2011

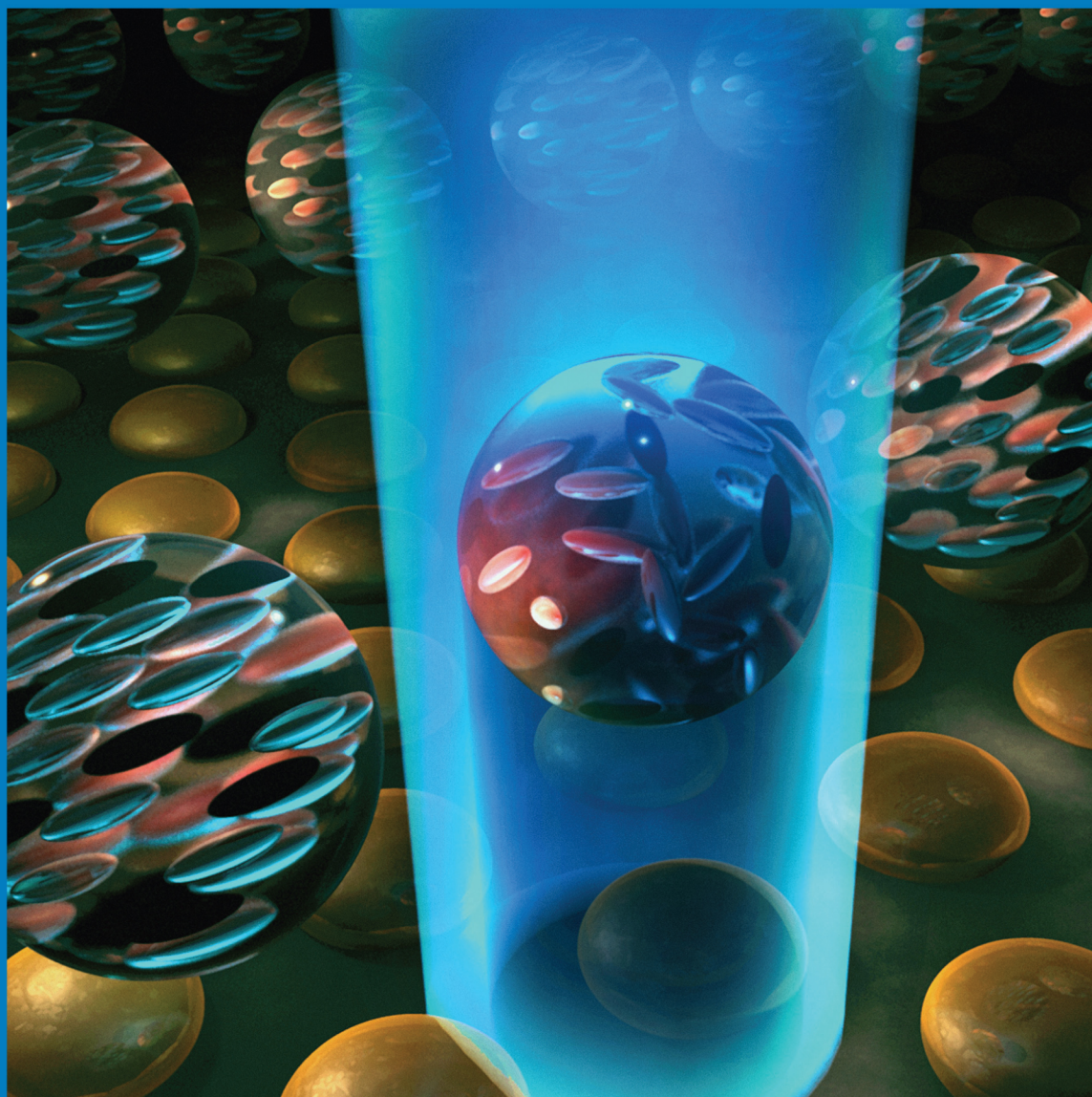
VOLUME 115

NUMBER 15

[pubs.acs.org/JPCCK](http://pubs.acs.org/JPCCK)

# THE JOURNAL OF PHYSICAL CHEMISTRY

C



All-Optical  
Manipulation  
of Liquid Crystal  
Alignment and  
Localized Surface  
Plasmon Coupling  
(see page 5A)

NANOMATERIALS, INTERFACES, HARD MATTER



ACS Publications

MOST TRUSTED. MOST CITED. MOST READ.

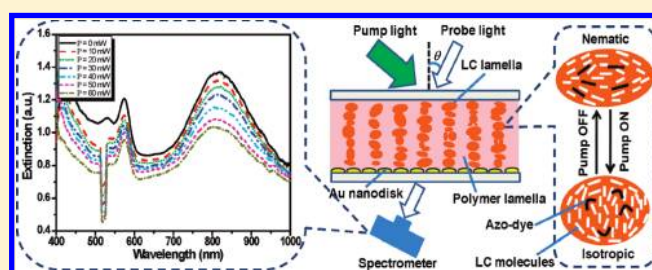
[www.acs.org](http://www.acs.org)

# All-Optical Modulation of Localized Surface Plasmon Coupling in a Hybrid System Composed of Photoswitchable Gratings and Au Nanodisk Arrays

Yan Jun Liu,<sup>†</sup> Yue Bing Zheng,<sup>†</sup> Justin Liou,<sup>†</sup> I-Kao Chiang,<sup>†</sup> Iam Choon Khoo,<sup>‡</sup> and Tony Jun Huang<sup>\*,†</sup>

<sup>†</sup>Department of Engineering Science and Mechanics and <sup>‡</sup>Department of Electrical Engineering, The Pennsylvania State University, University Park, Pennsylvania 16802, United States

**ABSTRACT:** We conduct a real-time study of all-optical modulation of localized surface plasmon resonance (LSPR) coupling in a hybrid system that integrates a photoswitchable optical grating with a gold nanodisk array. This hybrid system enables us to investigate two important interactions: (1) LSPR-enhanced grating diffraction and (2) diffraction-mediated LSPR in the Au nanodisk array. The physical mechanism underlying these interactions was analyzed and experimentally confirmed. With its advantages in cost-effective fabrication, easy integration, and all-optical control, the hybrid system described in this work could be valuable in many nanophotonic applications.



## 1. INTRODUCTION

Plasmonics paves the way for manipulating optical signals at the nanoscale by coupling light to coherent electronic excitations (known as surface plasmon resonances) at the interface between dielectric materials and metal nanostructures.<sup>1–9</sup> The strong confinement of light associated with surface plasmon resonances has led to the development of various subwavelength photonic components, such as waveguides,<sup>10,11</sup> switches,<sup>12–14</sup> filters,<sup>15–17</sup> lenses,<sup>18–21</sup> microscopies,<sup>22,23</sup> and spasers.<sup>24–27</sup> Gratings have been used to efficiently couple free-space light to surface plasmons by bridging the momentum gap between them.<sup>28,29</sup> Conversely, surface plasmons can also enhance the grating diffraction.<sup>30–34</sup> Interactions at the interface between a grating and metal nanostructure are complicated and have attracted intensive attention.<sup>30–34</sup> A better understanding of these interactions relies on the capability to continuously tune either the grating period or metallic nanostructure size, thus achieving interactions at different plasmon resonances or diffraction wavelengths.

Until now, tuning has been achieved by producing a series of samples with different metal nanostructures or grating periods; this approach has caused poor experimental reproducibility and unreliable comparisons among different samples.<sup>35,36</sup> To address these problems, we develop a hybrid system that integrates a photoswitchable grating and a Au nanodisk array. In this system, the diffraction of the grating can be continuously tuned in real time by an external pump light. This tunable system allows us to study the interactions between the grating and Au nanodisk array in real time. These interactions include the localized surface plasmon resonance (LSPR)-enhanced diffraction of the grating and diffraction-mediated LSPR of the Au nanodisk array.

In this hybrid system, the photoswitchable grating was produced from azo-dye-doped holographic polymer-disperse liquid crystals (HPDLC).<sup>37</sup> HPDLC-based material systems<sup>38</sup> have been extensively investigated for photonic applications due to the LC's unique optical properties.<sup>39–49</sup> The one-step, large-area, simple fabrication process of HPDLC-based devices makes them convenient for integration with other systems to realize synergic functions. In this experiment, we bound an HPDLC-based switchable grating onto a Au nanodisk array and demonstrated that the trans–cis transformation of the azo dyes embedded in the grating structure results in the nematic–isotropic (N–I) phase transition of the liquid crystals (LCs),<sup>50,51</sup> thus changing the plasmonic properties of the Au nanodisk array. Compared with existing counterparts driven electrically<sup>52–55</sup> or chemically,<sup>56</sup> the light-driven system demonstrated here can be conveniently integrated with other nanophotonic devices and become an integral component for future all-optical plasmonic systems.

## 2. EXPERIMENTAL SECTION

Azo-dye-doped HPDLC structures were fabricated from a standard prepolymer syrup containing 40.67 wt % monomer, dipentaerythritol penta-/hexa-acrylate (DPPHA); 6.74 wt % cross-linking monomer, *N*-vinylpyrrolidone (NVP); 0.71 wt % photoinitiator, Rose Bengal (RB); 0.76 wt % co-initiator, *N*-phenylglycine (NPG); 7.64 wt % surfactant, oleic acid (OA); 0.86 wt % azo-dye, methyl red (MR); and 42.63 wt % LC E7. The LC E7 was purchased from Merck, and the other materials were

**Received:** November 26, 2010

**Revised:** January 11, 2011

**Published:** March 04, 2011



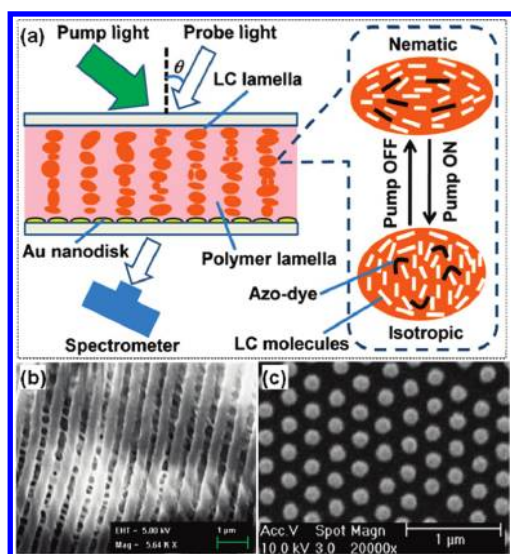


**Figure 1.** (a) Schematic of the experimental setup to characterize the LSPR modulation. The enlarged part showing the N–I phase transition induced by the trans–cis photoisomerization of the azo dye, (b) SEM image illustrating the morphology of the azo-based HPDLC transmission grating and (c) SEM image of a Au nanodisk array hexagonally arranged on a glass substrate.

purchased from Sigma-Aldrich. The prepolymer and LC were mechanically blended at 65 °C (slightly higher than the clearing point of the LC) to form a homogeneous mixture. Drops of the mixture were sandwiched between two glass slides. The thickness of the samples was controlled to be  $\sim 10 \mu\text{m}$  using plastic microbeads as spacers between the two glass slides. Bragg transmission gratings were prepared using two intersected collimated laser beams (wavelength, 488 nm; angle,  $\sim 40^\circ$ ) at room temperature. This produced a one-dimensional periodic structure with the grating vector parallel to the surface of the cell. The diffraction efficiency of these gratings was measured using a p-polarized He–Ne laser (633 nm).

Once the grating was formed, we removed one of the substrates and bound the exposed HPDLC film to the Au nanodisk plate with physical contact for characterization. We irradiated the grating with a p-polarized, pulsed  $\text{Ar}^+$  laser beam (514.5 nm) with a pulse duration of  $\sim 10$  s. The extinction spectra of the composite structure (Au nanodisk + HPDLC grating) were monitored with an unpolarized white-light beam (HR4000CG-UV-NIR, Ocean Optics) that was incident upon the grating at an angle of  $42^\circ$ . The unfocused pumping beam had a diameter of  $\sim 5$  mm; the diameter of the probe beam was  $\sim 2$  mm to ensure that it was completely covered by the pumping beam. The extinction spectra of a pure grating and a bare gold nanodisk plate were also monitored using the same procedure in control experiments. The response times for the “ON” and “OFF” photoswitching processes were measured using a near-infrared semiconductor laser (808 nm). By manually blocking the pumping light, the responses were recorded by an oscilloscope.

### 3. RESULTS AND DISCUSSION

Figure 1a shows the schematic of the experimental setup. An azo-based HPDLC transmission grating with alternating polymer-rich and LC-rich lamella was produced through holographic photopolymerization. Due to the shrinkage of the polymer

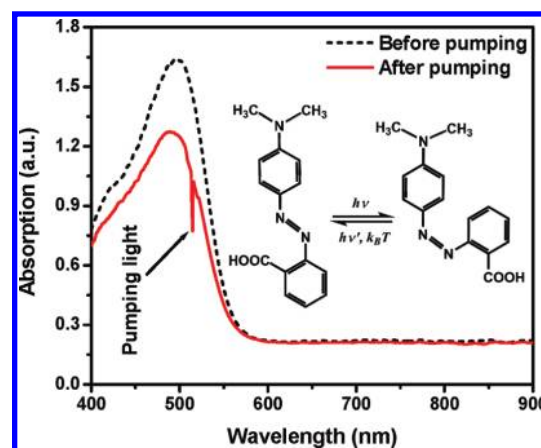


**Figure 2.** The trans–cis isomerization of MR in acetone solution under the pumping light with the wavelength of 514.5 nm. The inset shows the chemical structure of a MR molecule and its reversible trans–cis isomerization.

during polymerization, the LC droplets are nematically ordered and their directors tend to align parallel to the grating vector direction.<sup>37</sup> The azo-dye used in the experiments was methyl red (MR). It is well-known that MR molecules undergo trans–cis isomerization under a visible light exposure (Figure 2).<sup>57</sup> Once the grating was fabricated, it was bound to a Au nanodisk array situated on a glass slide. When the whole device was illuminated by the laser beam, the azo dyes experienced the trans–cis photoisomerization, which triggered the N–I phase transition of the LC molecules. In addition, upon light irradiation, the grating structure, especially its polymer-rich regions, could be subject to thermal expansion caused by laser heating of the grating structure.<sup>58</sup> This subsequently squeezed the LC droplets, causing them to deform from ellipsoids to more-spherical shapes (Figure 1a inset). It is worth noting that the heating effect does not induce any detectable temperature change, indicating that temperature has little contribution to the N–I phase transition of the LC. Figure 1b shows a typical scanning electron microscopy (SEM) image of the transmission grating with the LCs removed. The grating period was estimated to be  $600 \pm 20$  nm. Au nanodisk arrays (Figure 1c) were fabricated on glass substrates using nanosphere lithography combined with two reactive ion etching steps.<sup>59,60</sup> The mean diameter and period of the hexagonally arranged Au nanodisk array were determined on the basis of a Gaussian fitting<sup>60</sup> to be  $150 \pm 14$  and  $320 \pm 32$  nm, respectively.

The extinction spectra before and after binding the nanodisks to the azo-based HPDLC grating structure were recorded with normally incident light, as shown in Figure 3. The solid curve represents the extinction spectrum of the bare Au nanodisk array in air, and the dashed curve represents the extinction spectrum after the nanodisk array was bound to the grating structure. In a previous report, Zheng and co-workers investigated the coupling effect between neighboring nanodisks in a similar hexagonally arranged Au nanodisk array.<sup>61</sup> Compared with a single Au nanodisk, the array has a narrower and higher-intensity LSPR peak due to a collective coupling effect. As a result, pronounced extinction peaks can be observed in both cases, corresponding to where the LSPR occurs.<sup>62</sup> After binding the nanodisks to the grating, the extinction peak red-shifted from 690 to 795 nm due to the increased refractive index of the surroundings. In addition, due to the periodic index modulation within the grating

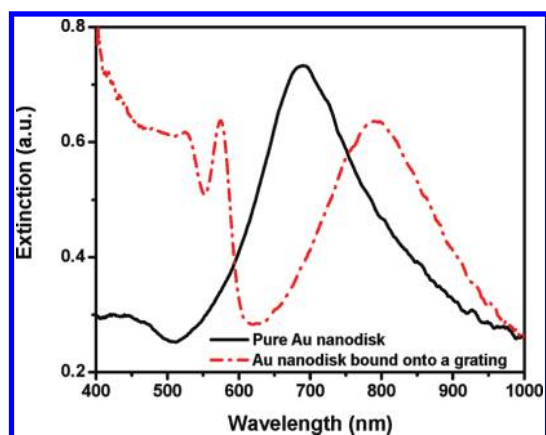


**Figure 3.** Extinction spectra of (a) a bare Au nanodisk array and (b) a Au nanodisk array bound onto an azo-based HPDLC grating.

structure, the intensity of the LSPR peak decreased, and the bandwidth increased. It is worth noting that the angle-dependent measurements of our Au nanodisk array show that the LSPR does not depend on the in-plane polarization of the incident light. Therefore, there is no preferred binding direction between the grating and Au nanodisk array.

Both the grating and the Au nanodisk array exhibited peaks in the extinction spectrum due to the grating diffraction and LSPR, respectively. Since they had different periods, their extinction spectra were not in the same spectral range under the same normally incident probe light. However, because the angular dependence of the azo-based HPDLC grating was much more sensitive than the Au nanodisk array, we could always adjust the incident angle to overlap the peaks from the HPDLC grating and the Au nanodisk array and enhance the effective extinction from the Au nanodisk array bound to the HPDLC grating. When the peaks overlap (at an incident angle of  $\sim 42^\circ$  in our experiment), maximum modulation of the extinction can be realized by modulating the grating. This modulation was accomplished by illuminating the system with a 514 nm laser to induce trans–cis isomerization of the MR, decrease LC order, and lower the index contrast between the LC and polymer regions of the grating. The effective extinction intensity of the composite structure (Au nanodisk + grating system) was thereby decreased.

Figure 4a shows the extinction spectra under different pumping intensities at an incident probe angle of  $42^\circ$ . In addition to a reduction in the peak extinction, we also observed an overall decrease in extinction between 400 and 600 nm caused by the increased cis population. For a comparison, we conducted a control experiment with the Au nanodisk array separated from the azo-based HPDLC grating (referred as uncoupled system, Figure 4b). In this case, the extinction peak was only the superposition of the distinct extinction spectra of the Au nanodisk array and the azo-based HPDLC grating (data not shown). The spectral changes in this case were contributed only from the diffraction switching of the grating. When the Au nanodisk array is bound to the azo-based HPDLC grating (referred as coupled system), the extinction peak intensity (Figure 4a) is higher than the uncoupled system (Figure 4b). Moreover, upon pumping, the modulation depth (intensity change) for the coupled system is larger than that of the uncoupled one. This difference is caused by the additional diffraction effect from an LSPR-induced absorption grating. Because the Au nanodisk array was covered by the grating with an alternating periodic refractive index, and the

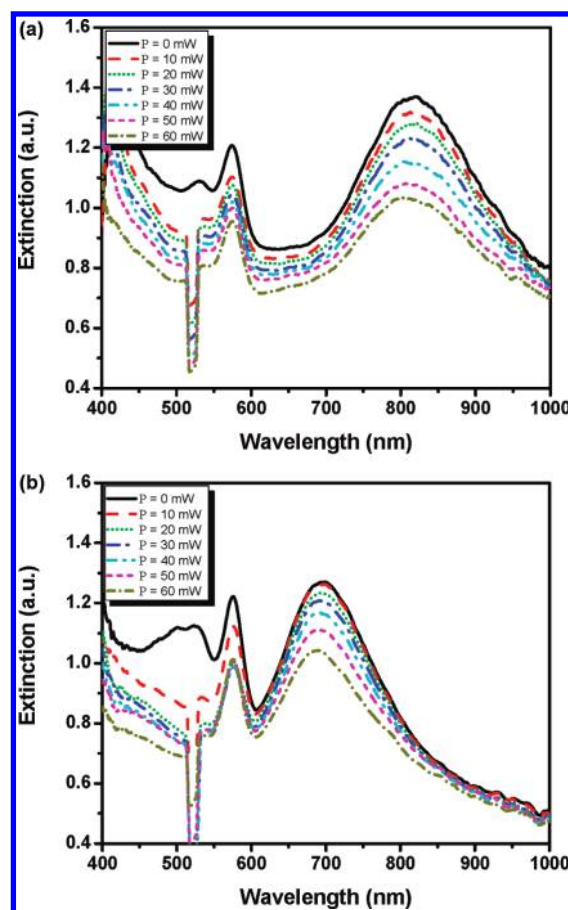


**Figure 4.** Extinction spectra at different pumping intensities for (a) the Au nanodisk array bound onto the azo-based HPDLC grating and (b) the Au nanodisk array separated from the azo-based HPDLC grating.

LSPR, which leads to optical absorption, of Au nanoparticles is strongly dependent on the surrounding refractive index, this coupled system would demonstrate periodic modulation in absorption. As a result, an absorption grating was formed.<sup>63,64</sup> This results in much more light diffracted in the vicinity of the LSPR peak.

To confirm this effect, experiments were carried out to compare the diffraction between the azo-based HPDLC grating and the coupled system. Due to the large dispersion of the light by the grating diffraction, only a small band of the diffraction was measured. Figure 5 shows that, due to the absorption of the Au nanodisks, the diffraction intensity outside the LSPR range was much lower than that of the bare grating. However, within the LSPR range, the diffraction intensity was higher in the coupled system. This observation is in good agreement with our proposed mechanism: due to the enhanced diffraction caused by the absorption grating, when the LSPR peak and the diffraction peak were overlapped, the extinction peak had higher intensity. In this case, when the coupled system was subject to exposure, the modulation depth became larger compared with that of the uncoupled system. Since surface plasmons usually localize at the interface with a range of less than 100 nm, only a very thin azo-based HPDLC film needs to be used to control the coupling between the LSPR and grating. The  $\sim 10\ \mu\text{m}$  thick HPDLC film was used in our experiments only for its easy fabrication and convenient binding to the gold substrate.

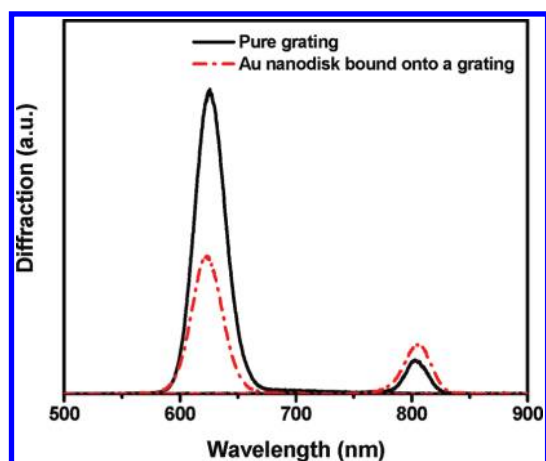


Figure 5. Comparison for the diffracted intensity of (a) a pure grating and (b) a grating bound onto a Au nanodisk array.

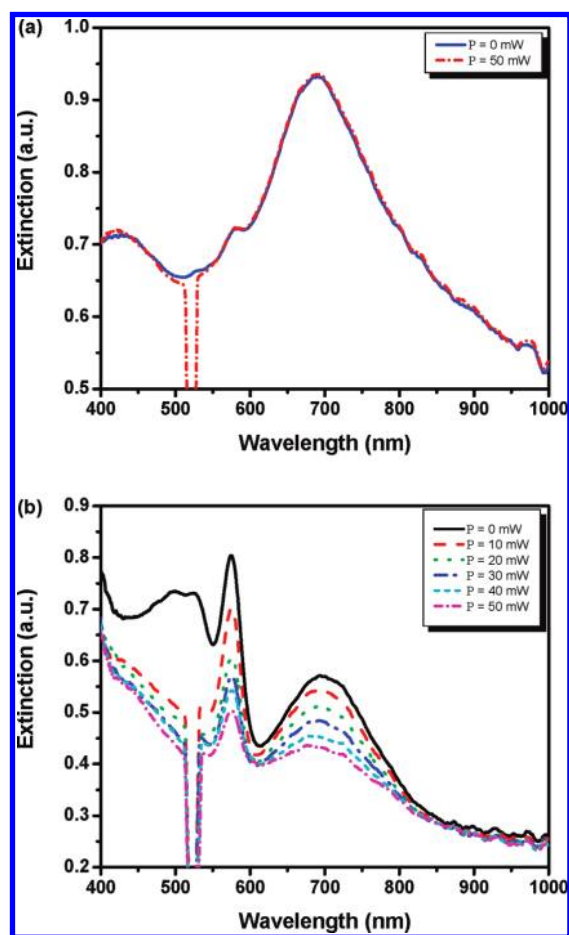


Figure 6. Control experiments under the photopumping for (a) a pure Au nanodisk array and (b) a pure grating.

For a comparison, we conducted control experiments in which the pure Au nanodisks (Figure 6a) and the pure grating (Figure 6b) were photopumped. Figure 6a shows that the photopump has no effect on the LSPR of the bare Au nanodisk array. In contrast, significant spectra changes can be observed under different pumping intensities for the azo-based HPDLC grating (Figure 6b), which was pumped at an incident angle

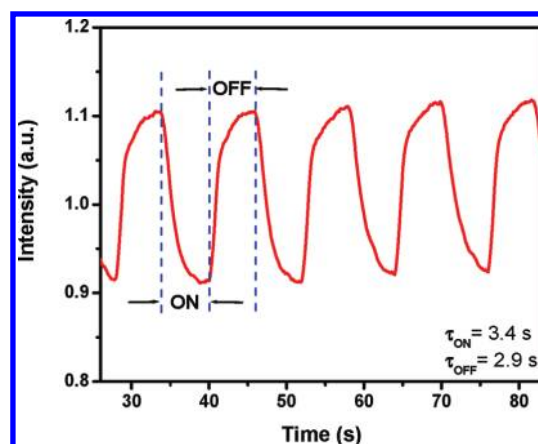


Figure 7. Time-dependent extinction changes for an azo-based HPDLC grating bound with a Au nanodisk array when the pump light was turned on and off alternatively.

of  $36^\circ$ . The change in the band (600–800 nm) was due to decreased diffraction from the grating caused by the N–I phase transition of the LCs. In this experiment, light propagating through the grating sees the LC droplets with an effective index, which is an average of the ordinary and extraordinary indices, and slightly higher than the isotropic index of the LC material. For an LC droplet, the maximum effective index of the nematic and isotropic states can be estimated approximately as  $n_N = [(n_o^2 + n_e^2)/2]^{1/2}$  and  $n_I = [(n_o^2 + n_o^2 + n_e^2)/3]^{1/2}$ , respectively. For LC E7, these values are  $n_N = 1.64$  and  $n_I = 1.60$ . The refractive index of the polymer matrix,  $n_p$ , is 1.53. For a  $10\text{-}\mu\text{m}$ -thick grating, this index change gave a  $\sim 30\%$  reduction of diffraction efficiency from the N–I phase transition of the LCs measured by a p-polarized He–Ne laser.<sup>37</sup>

Reversible modulation of the LSPR for the HPDLC grating sample bound with Au nanodisk arrays was achieved by switching the pump light on and off (Figure 7). The response times for the “ON” and “OFF” photoswitching processes were estimated to be 3.4 and 2.9 s, respectively. Because the response time of our system is influenced by multiple factors, including grating structure, working temperature, the amount of azo dyes, and the power of the pump light, optimization of these factors will be investigated further to improve response times.

For most azobenzene derivatives, UV light is needed to trigger the trans–cis isomerization.<sup>65,66</sup> However, long-time UV pumping may greatly degrade the physical properties of the LCs, including clearing temperature, birefringence, dielectric constants, and the viscoelastic coefficient.<sup>67</sup> In our azo-based HPDLC material system, the green light (514.5 nm) was used to trigger the trans–cis isomerization because the absorption band of trans-isomer is typically in the blue-green range,<sup>57</sup> where the pumping light has a negligible effect on the LCs. Therefore, our material system will have a longer lifetime than that of other material systems that use UV light pumps.

#### 4. CONCLUSION

In summary, we have studied all-optical modulation of LSPR coupling in a hybrid system consisting of an azo-based, photo-switchable HPDLC transmission grating bound to a Au nanodisk array. Two important interaction scenarios were observed: 1) LSPR-enhanced diffraction of the grating, and 2) diffraction-mediated LSPR of the Au nanodisk array. As a pumping laser



incident upon the device was turned on and off, a reversible modulation of the LSPR intensity was achieved. The underlying mechanism is the phase transition of the LCs in the HPDLC grating triggered by the trans–cis isomerization of the azo molecules, resulting in photoswitched diffraction: a combination of the absorption grating enhanced diffraction induced by the LSPR excitation and self-diffraction of the grating. The optical switching performance could be further improved by using different azo-dyes or polymer LC polymer slices (POLYCRYPS) structures.<sup>68,69</sup> This hybrid system is potentially useful in many plasmonic applications, such as storage, filters, and communications.

## AUTHOR INFORMATION

### Corresponding Author

\*E-mail: junhuang@psu.edu.

## ACKNOWLEDGMENT

The authors thank Aitan Lawit and Brian Kiraly for helpful discussion and manuscript preparation. This work was supported by the Air Force Office of Scientific Research (FA9550-08-1-0349), NIH Director's New Innovator Award (1DP2OD007209-01), the Army Research Office, the National Science Foundation (ECCS-0801922 and ECCS-0609128), and the Penn State Center for Nanoscale Science (MRSEC). Components of this work were conducted at the Penn State node of the NSF-funded National Nanotechnology Infrastructure Network.

## REFERENCES

- Ozbay, E. *Science* **2006**, *311*, 189.
- Maier, S. A.; Brongersma, M. L.; Kik, P. G.; Meltzer, S.; Requicha, A. A. G.; Atwater, H. A. *Adv. Mater.* **2001**, *13*, 1501.
- Atwater, H. A.; Maier, S.; Polman, A.; Dionne, J. A.; Sweatlock, L. *MRS Bull.* **2005**, *30*, 385.
- Haes, A. J.; Zhao, J.; Zou, S. L.; Own, C. S.; Marks, L. D.; Schatz, G. C.; Van Duyne, R. P. *J. Phys. Chem. B* **2005**, *109*, 11158.
- McMahon, J. M.; Wang, Y. M.; Sherry, L. J.; Van Duyne, R. P.; Marks, L. D.; Gray, S. K.; Schatz, G. C. *J. Phys. Chem. C* **2009**, *113*, 2731.
- Chen, H. J.; Shao, L.; Woo, K. C.; Ming, T.; Lin, H.-Q.; Wang, J. F. *J. Phys. Chem. C* **2009**, *113*, 17691.
- Ringe, E.; McMahon, J. M.; Sohn, K.; Cogley, C.; Xia, Y. N.; Huang, J. X.; Schatz, G. C.; Marks, L. D.; Van Duyne, R. P. *J. Phys. Chem. C* **2010**, *114*, 12511.
- Khatua, S.; Manna, P.; Chang, W.-S.; Tcherniak, A.; Friedlander, E.; Zubarev, E. R.; Link, S. J. *J. Phys. Chem. C* **2010**, *114*, 7251.
- Dridi, M.; Vial, A. J. *J. Phys. Chem. C* **2010**, *114*, 9541.
- Quinten, M.; Leitner, A.; Krenn, J. R.; Aussenegg, F. R. *Opt. Lett.* **1998**, *23*, 1331.
- Maier, S. A.; Kik, P. G.; Atwater, H. A.; Meltzer, S.; Harel, E.; Koel, B. E.; Requicha, A. A. G. *Nat. Mater.* **2003**, *2*, 229.
- Hsiao, V. K. S.; Zheng, Y. B.; Juluri, B. K.; Huang, T. J. *Adv. Mater.* **2008**, *20*, 3528.
- Liu, Y. J.; Hao, Q. Z.; Smalley, J. S. T.; Liou, J.; Khoo, I. C.; Huang, T. J. *Appl. Phys. Lett.* **2010**, *97*, 091101.
- Ming, T.; Zhao, L.; Xiao, M. D.; Wang, J. F. *Small* **2010**, *6*, 2514.
- Ebbesen, T. W.; Lezec, H. J.; Ghaemi, H. F.; Thio, T.; Wolff, P. A. *Nature* **1998**, *391*, 667.
- Genet, C.; Ebbesen, T. W. *Nature* **2007**, *445*, 39.
- Lezec, H. J.; Degiron, A.; Devaux, E.; Linke, R. A.; Martin-Moreno, L.; Garcia-Vidal, F. J.; Ebbesen, T. W. *Science* **2002**, *297*, 820.
- Fang, N.; Lee, H.; Sun, C.; Zhang, X. *Science* **2005**, *308*, 534.
- Liu, Z.; Lee, H.; Xiong, Y.; Sun, C.; Zhang, X. *Science* **2007**, *315*, 1686.
- Srituravanich, W.; Pan, L.; Wang, Y.; Sun, C.; Bogy, D. B.; Zhang, X. *Nat. Nanotechnol.* **2008**, *3*, 733.
- Zhao, Y. H.; Lin, S. S.-C.; Nawaz, A. A.; Kiraly, B.; Hao, Q. Z.; Liu, Y. J.; Huang, T. J. *Opt. Express* **2010**, *18*, 23458.
- Hu, H.; Ma, C.; Liu, Z. *Appl. Phys. Lett.* **2010**, *96*, 113107.
- Wei, F.; Liu, Z. *Nano Lett.* **2010**, *10*, 2531.
- Bergman, D. J.; Stockman, M. I. *Phys. Rev. Lett.* **2003**, *90*, 027402.
- Seidel, J.; Grafstrom, S.; Eng, L. *Phys. Rev. Lett.* **2005**, *94*, 177401.
- Noginov, M. A.; Zhu, G.; Mayy, M.; Ritzo, B. A.; Noginova, N.; Podolskiy, V. A. *Phys. Rev. Lett.* **2008**, *101*, 226806.
- Zheludev, N. I.; Prosvirnin, S. L.; Papasimakis, N.; Fedotov, V. A. *Nat. Photon.* **2008**, *2*, 351.
- Kocabas, A.; Dana, A.; Aydinli, A. *Appl. Phys. Lett.* **2006**, *89*, 041123.
- MacDonald, K. F.; Samson, Z. L.; Stockman, M. I.; Zheludev, N. I. *Nat. Photon.* **2009**, *3*, 55.
- Yu, F.; Tian, S. J.; Yao, D. F.; Knoll, W. *Anal. Chem.* **2004**, *76*, 3530.
- Tian, S. J.; Armstrong, N. R.; Knoll, W. *Langmuir* **2005**, *21*, 4656.
- Wark, A. W.; Lee, H. J.; Qavi, A. J.; Corn, R. M. *Anal. Chem.* **2007**, *79*, 6697.
- Singh, B. K.; Hillier, A. C. *Anal. Chem.* **2008**, *80*, 3803.
- Yeh, W.-H.; Kleingartner, J.; Hillier, A. C. *Anal. Chem.* **2010**, *82*, 4988.
- Juluri, B. K.; Zheng, Y. B.; Ahmed, D.; Jensen, L.; Huang, T. J. *J. Phys. Chem. C* **2008**, *112*, 7309.
- Lu, J.; Petre, C.; Yablonovitch, E.; Conway, J. J. *Opt. Soc. Am. B* **2007**, *24*, 2268.
- Liu, Y. J.; Zheng, Y. B.; Shi, J.; Huang, H.; Walker, T. R.; Huang, T. J. *Opt. Lett.* **2009**, *34*, 2351.
- Bunning, T. J.; Natarajan, L. V.; Tondiglia, V. P.; Sutherland, R. L. *Annu. Rev. Mater. Sci.* **2000**, *30*, 83.
- Caputo, R.; De Sio, L.; Veltri, A.; Umerton, C.; Sukhov, A. V. *Opt. Lett.* **2004**, *29*, 1261.
- Liu, Y. J.; Sun, X. W.; Liu, J. H.; Dai, H. T.; Xu, K. S. *Appl. Phys. Lett.* **2005**, *86*, 041115.
- Vita, F.; Marino, A.; Tkachenko, V.; Abbate, G.; Lucchetta, D. E.; Criante, L.; Simoni, F. *Phys. Rev. E* **2005**, *72*, 011702.
- Liu, Y. J.; Sun, X. W.; Shum, P.; Li, H. P.; Mi, J.; Ji, W.; Zhang, X. H. *Appl. Phys. Lett.* **2006**, *88*, 061107.
- Liu, Y. J.; Sun, X. W.; Elim, H. I.; Ji, W. *Appl. Phys. Lett.* **2007**, *90*, 011109.
- Liu, Y. J.; Sun, X. W. *Appl. Phys. Lett.* **2006**, *89*, 171101.
- Liu, Y. J.; Sun, X. W. *Jpn. J. Appl. Phys.* **2007**, *46*, 6634.
- Shi, J.; Hsiao, V. K. S.; Huang, T. J. *Nanotechnology* **2007**, *18*, 465501.
- Hsiao, V. K. S.; Waldeisen, J. R.; Zheng, Y.; Lloyd, P. F.; Bunning, T. J.; Huang, T. J. *J. Mater. Chem.* **2007**, *17*, 4896.
- Fritz, K. P.; Scholes, G. D. *J. Phys. Chem. B* **2003**, *107*, 10141.
- Lamm, R. K.; Fritz, K. P.; Scholes, G. D.; Barbara, P. F. *J. Phys. Chem. B* **2004**, *108*, 4593.
- Khoo, I. C.; Park, J. H.; Liou, J. D. *J. Opt. Soc. Am. B* **2008**, *25*, 1931.
- Khoo, I. C. *Phys. Rep.* **2009**, *471*, 221.
- Muller, J.; Sonnichsen, C.; von Poschinger, H.; von Plessen, G.; Klar, T. A.; Feldmann, J. *Appl. Phys. Lett.* **2002**, *81*, 171.
- Kossyrev, P. A.; Yin, A. J.; Cloutier, S. G.; Cardimona, D. A.; Huang, D. H.; Alsing, P. M.; Xu, J. M. *Nano Lett.* **2005**, *5*, 1978.
- Chu, K. C.; Chao, C. Y.; Chen, Y. F.; Wu, Y. C.; Chen, C. C. *Appl. Phys. Lett.* **2006**, *89*, 103107.
- Dickson, W.; Wurtz, G. A.; Evans, P. R.; Pollard, R. J.; Zayats, A. V. *Nano Lett.* **2008**, *8*, 281.
- Zheng, Y. B.; Yang, Y.-W.; Jensen, L.; Fang, L.; Juluri, B. K.; Flood, A. H.; Weiss, P. S.; Stoddart, J. F.; Huang, T. J. *Nano Lett.* **2009**, *9*, 819.
- Lee, G. J.; Kim, D.; Lee, M. *Appl. Opt.* **1995**, *34*, 138.
- Fuh, A. Y.-G.; Tsai, M.-S.; Huang, L.-J.; Liu, T.-C. *Appl. Phys. Lett.* **1999**, *74*, 2572.

- (59) Zheng, Y. B.; Huang, T. J.; Desai, A. Y.; Wang, S. J.; Tan, L. K.; Gao, H.; Huan, A. C. H. *Appl. Phys. Lett.* **2007**, *90*, 183117.
- (60) Zheng, Y. B.; Juluri, B. K.; Mao, X.; Walker, T. R.; Huang, T. J. *J. Appl. Phys.* **2008**, *103*, 014308.
- (61) Zheng, Y. B.; Juluri, B. K.; Jensen, L. L.; Ahmed, D.; Lu, M. Q.; Jensen, L.; Huang, T. J. *Adv. Mater.* **2010**, *22*, 3603.
- (62) Hutter, E.; Fendler, J. H. *Adv. Mater.* **2004**, *16*, 1685.
- (63) Hung, W.-C.; Cheng, W.-H.; Tsai, M.-S.; Juan, Y.-C.; Jiang, I.-M.; Yeh, P. *Appl. Phys. Lett.* **2007**, *90*, 183115.
- (64) Hung, W.-C.; Cheng, W.-H.; Lin, Y.-S.; Jang, D.-J.; Jiang, I.-M.; Tsai, M.-S. *J. Appl. Phys.* **2008**, *104*, 063106.
- (65) Urbas, A.; Tondiglia, V.; Natarajan, L.; Sutherland, R.; Yu, H.; Li, J.-H.; Bunning, T. J. *Am. Chem. Soc.* **2004**, *126*, 13580.
- (66) Urbas, A.; Klosterman, J.; Tondiglia, V.; Natarajan, L.; Sutherland, R.; Tsutsumi, O.; Ikida, T.; Bunning, T. *Adv. Mater.* **2004**, *16*, 1453.
- (67) Wen, C.-H.; Gauza, S.; Wu, S.-T. *Liq. Cryst.* **2004**, *31*, 1479.
- (68) De Sio, L.; Veltri, A.; Umeton, C.; Serak, S.; Tabiryan, N. *Appl. Phys. Lett.* **2008**, *93*, 181115.
- (69) De Sio, L.; Serak, S.; Tabiryan, N.; Ferjani, S.; Veltri, A.; Umeton, C. *Adv. Mater.* **2010**, *22*, 2316.